GMC STUDIES ON MEDIUM AND LONG RANGE FORECASTING AT GLA

E. Kalnay, R. Livezey, J. Pfaendtner, and Y. Sud
NASA/Goddard Laboratory for Atmospheres
Greenbelt, U.S.A.

ABSTRACT

This paper contains a brief review of results of GCM experiments on long range forecasting performed at the Experimental Climate Forecast Center (XCFC) of the Goddard Laboratory for Atmospheres (GLA). The GLA Fourth Order GCM climatology, derived from 6 winter and 4 summer 45-day integrations is presented. The skill of the 15-day averages of these benchmark integrations is also briefly discussed. Other subjects reviewed include: a successful attempt to "forecast forecast skill" in medium range forecasting; several studies of the predictability and the mechanisms involved in the maintenance of persistent anomalies in both the Northern and the Southern Hemisphere; a GCM/theoretical study that relates tropical sea surface temperature (SST) anomalies to precipitation anomalies; a study of the scale dependance of error growth and dynamic predictability; and other related work in progress.

1. INTRODUCTION

An Experimental Climate Forecast Center (XCFC) was established in 1982 at the Goddard Laboratory for Atmospheres (GLA, formerly known as GLAS), through an agreement between GLA and the National Climate Program Office, and is currently headed by R. Livezey. The XCFC, draws on the strong experience developed at GLA over a number of years in the areas of general circulation modeling, medium range forecasting, dynamic meteorology, and use of satellite data. The goal of XCFC is "to explore systematically

the existence, if any, of atmospheric predictability in the monthly to seasonal time scale by means of the use of comprehensive atmospheric models, and with emphasis on a priori estimates of forecast skill". In addition, it encompasses research efforts in areas such as the study of large-scale circulation anomalies from past conventional and satellite data, and coupled ocean-atmosphere models. Some of the resources available at the XCFC are the GLA Fourth Order GCM (Kalnay et al., 1983) which is generally used with a standard resolution of 4° lat, 5° lon and 9 equally spaced levels, the GLA Analysis/Forecast System (Baker, 1983, Baker et al., 1986), and the GLA Satellite Temperature Retrieval System (Susskind et al., 1983; Susskind and Reuter, 1985).

This paper contains a brief review of several GCM studies already completed (Sections 2 to 6) and related work in progress (Section 7).

2. BASELINE 45-DAY INTEGRATIONS

We are currently performing a series of experiments on long range forecasting which consist of the following:

a) Baseline experimental integrations with climatological boundary conditions.

This is a set of 6 winter and 6 summer 45-day integrations started from December 15 and June 15 of 1978-1984 respectively. These integrations have a two-fold purpose. First, to establish the climatology of GLA Fourth Order GCM, which so far has been used mostly for medium range forecasting. The second purpose is to determine the baseline level of predictability that can be expected from information on the initial conditions only.

b) Ensemble of 30-day forecasts performed using observed boundary conditions. We plan to perform sets of at least 6 winter and 6 summer ensembles with initial conditions corresponding to 3 consecutive days. The purpose of these experiments is again two-fold. First, to estimate the increase in predictability that can be assigned to the use of boundary anomalies both with or without error (SST, sea ice, albedo, soil moisture). Second, to explore the advantages of the use of Lagged Average Forecasting (Hoffman and Kalnay, 1986), as well as the a priori estimation of the forecast skill, using techniques similar to those described in the next section.

So far, we have only completed 6 winter baseline integrations (started from 15 December 1978-1983) and 4 summer integrations (from 15 June 1979, 1980, 1982 and 1983). Initial conditions were obtained from NMC and ECMWF analyses. We have not yet performed long integrations from our own analysis, except for the results described in Section 4. The results presented here and only preliminary, since we have not yet performed complete verifications, and several minor problems have been encountered in the initial conditions used for integrations and in the verification data.

2.1 Model Climatology

We present now the model January and July climatology, obtained by averaging the last 30 days of the 45-day integrations corresponding to different years. The winter average includes 6 integrations and the summer 4 integrations.

Figures 2.1 a, b, c, d represent the winter averages of Sea Level Pressure (SLP), 500 mb geopotential heights (ϕ), 200 mb ϕ and total precipitation respectively. Even though there are several deficiencies (e.g., surface lows are weak in the southern hemisphere, Siberian high is too weak), these fields are generally quite realistic and reproduce well most of the atmospheric stationary waves. Figures 2.2 a, b, c, d represent the corresponding summer averages. Again, the fields are generally realistic with some significant exceptions (e.g., unrealistic precipitation in the Saharan region of Africa, excessive precipitation over the continents in the summer, and weak southern hemisphere high latitude lows).

2.2 Baseline Predictability

Figures 2.3 to 2.7 present the first 15-day GLA forecasts and the NMC analyses anomalies with respect to their own average corresponding to 15-20 December of the years 1978 through 1982 respectively (the 1983 analysis was not available at the time of this writing). The anomaly correlations between these fields between 20° and 80° latitude are also indicated for both the Northern and Southern Hemispheres. Figures 2.8 to 2.12 present the same anomaly fields for the second 15-day averages, corresponding to the first half of the January of 1979 through 1983 respectively. The results corresponding to the last 15-day averages of the 45-day integrations are not presented because of their evident lack of skill. The winter anomaly correlation averages and standard deviations (in parentheses) are presented in Table 2.1. The results indicate that the skill in predicting the first 15-day average, measured by the anomaly correlations, is virtually the same in the Southern Hemisphere as in the Northern Hemisphere (0.57 versus 0.61 at 500 mb). The skill in the second 15-days is on the average

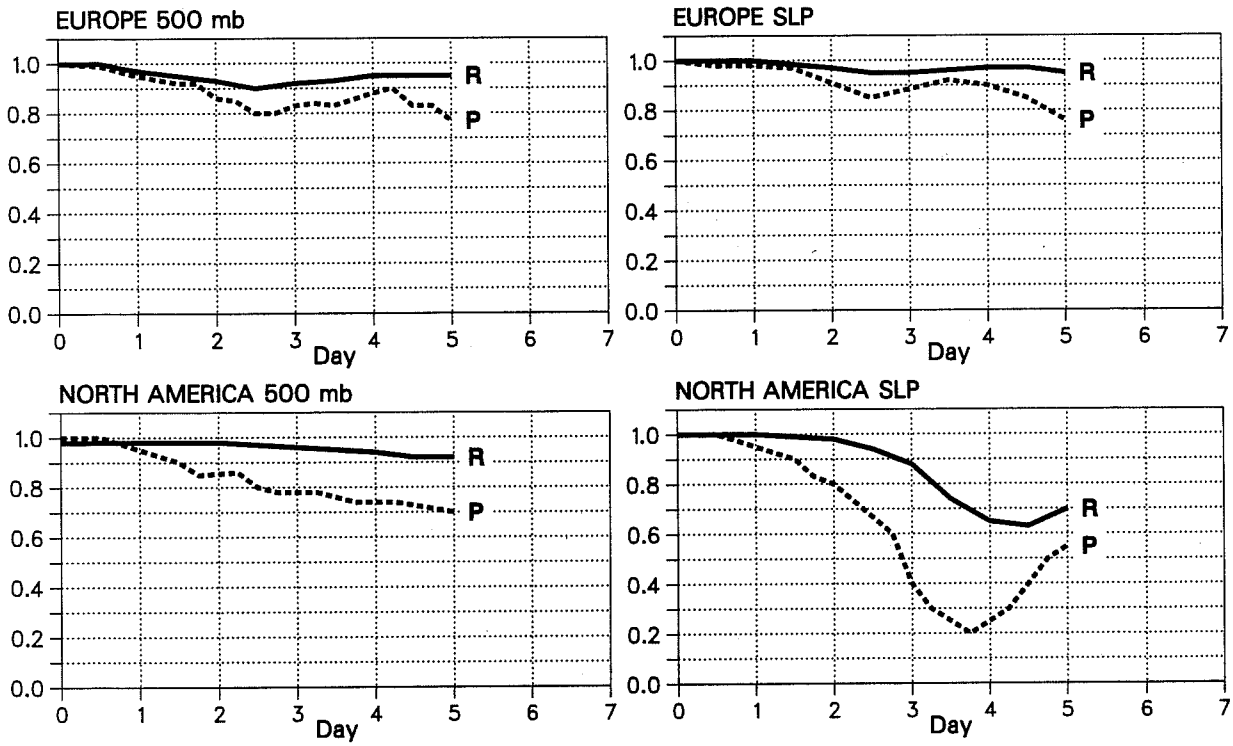

Fig. 3.1: Forecast/analysis anomaly correlation (ρ) and average forecast/forecast correlation (R) for the forecast from 21 Jan 1979, verified over Europe and North America, SLP and 500 mb.

	>5 days predicted	<5 days breakdown
>5 days observed	55	11
Breakdown <5 days	7	39

Table 3.1: Contingency table indicating the proportion of forecasts which remained skillful ($\rho \geq 0.60$) for more than five days among those predicted to remain skillful beyond five days. The table includes 14 forecasts verified over four regions, both at 500 mb and sea level pressure (SLP).

North America		Europe		North Atlantic		North Pacific	
8	4	14	1	19	1	14	5
2	14	2	11	2	6	1	8

Table 3.2: Same as Table 3.1 but for the individual regions.

Northern Hemisphere	
11	7
7	3

Table 3.3: Same as Table 3.1 but for the whole extratropical Northern Hemisphere.

Fig. 2.1 (top) and 2.2 (bottom): JANUARY and JULY model climatology.

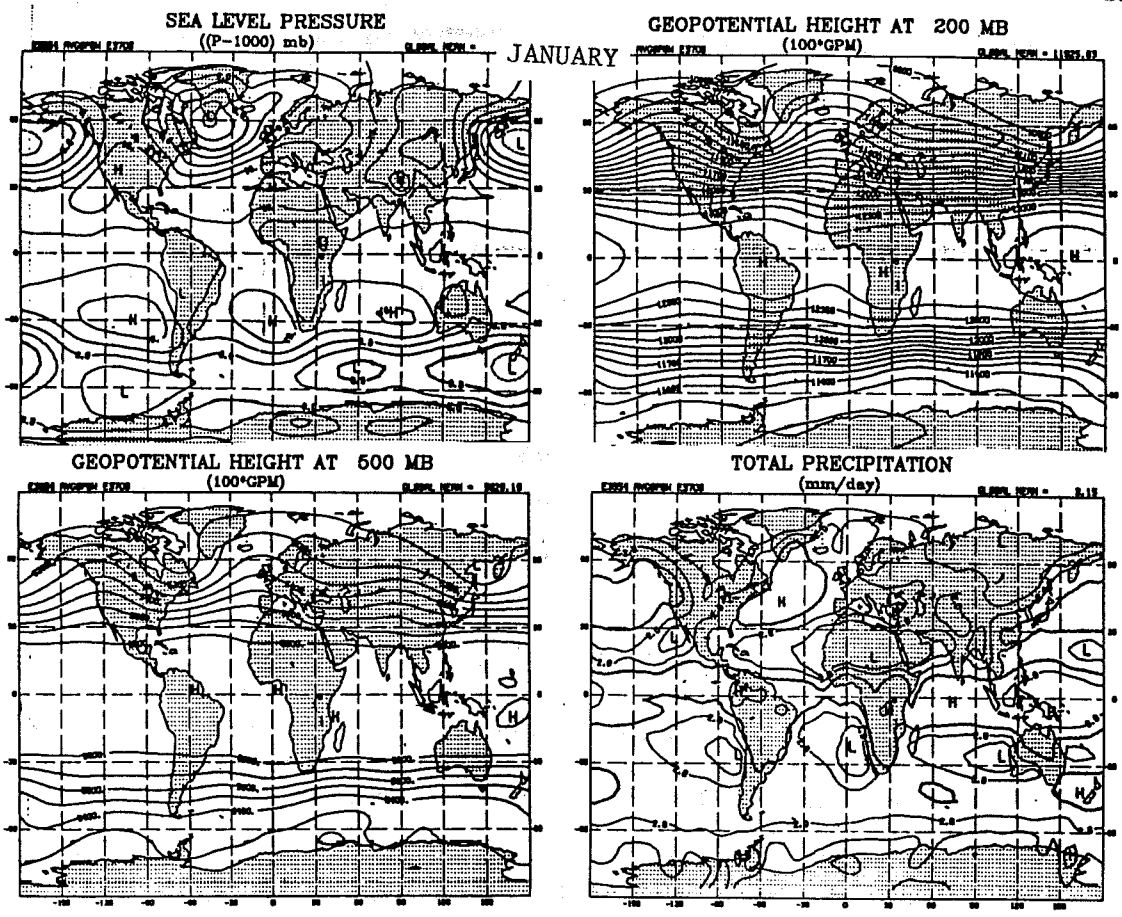

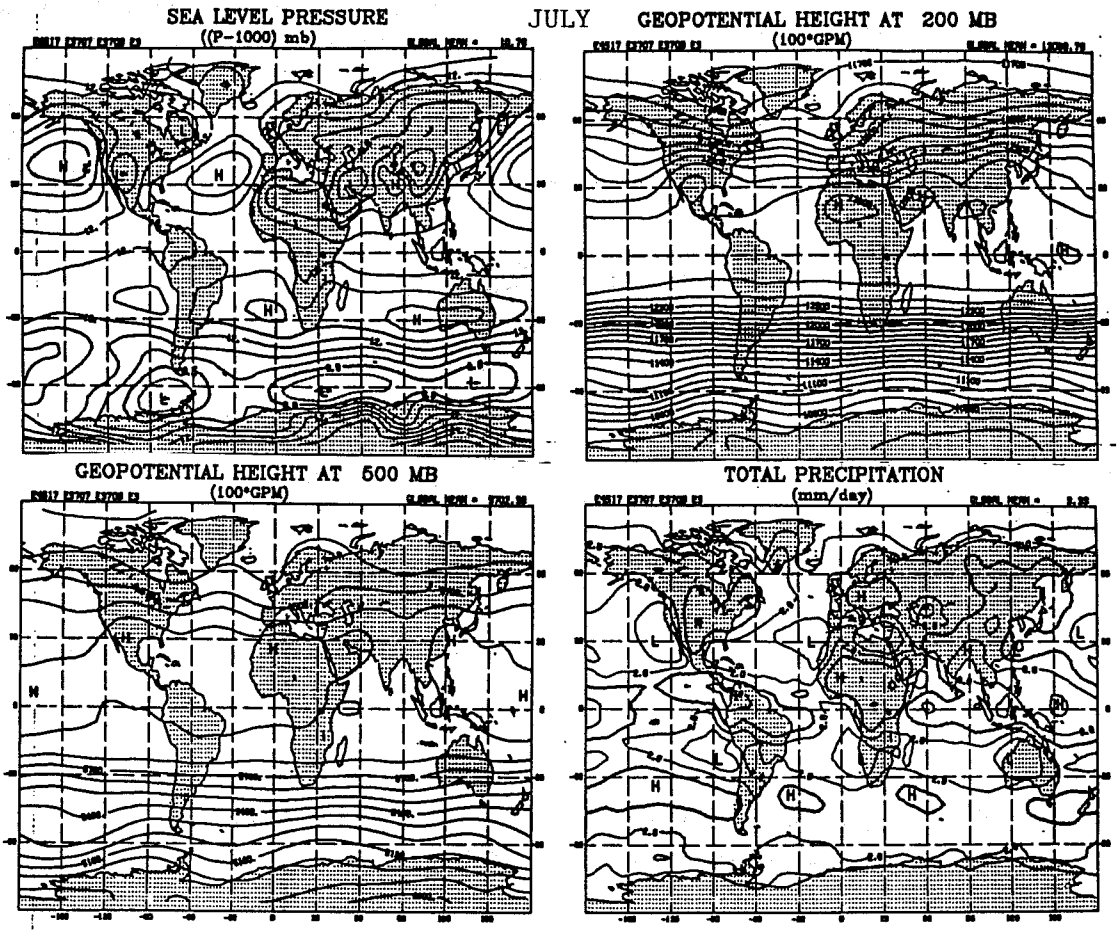

ρ=0.50

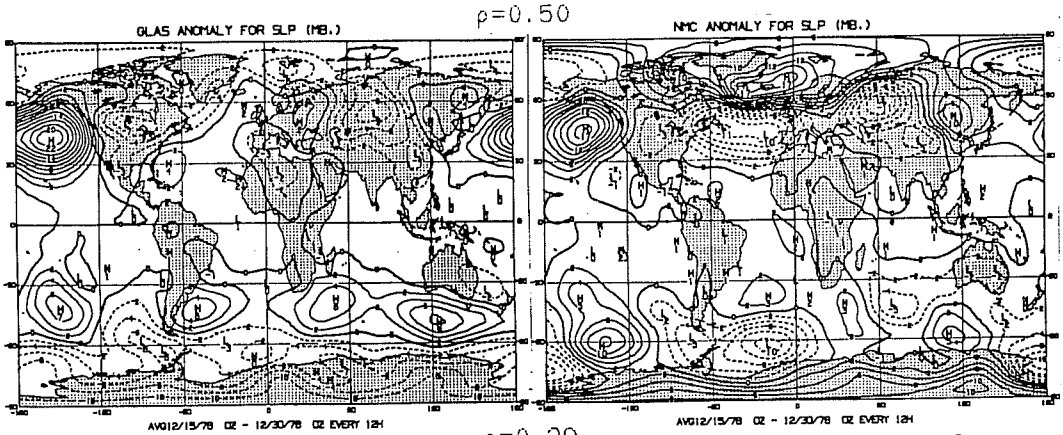

ρ=0.29

15/12/78-30/12/78

Fig. 2.3

ρ=0.69

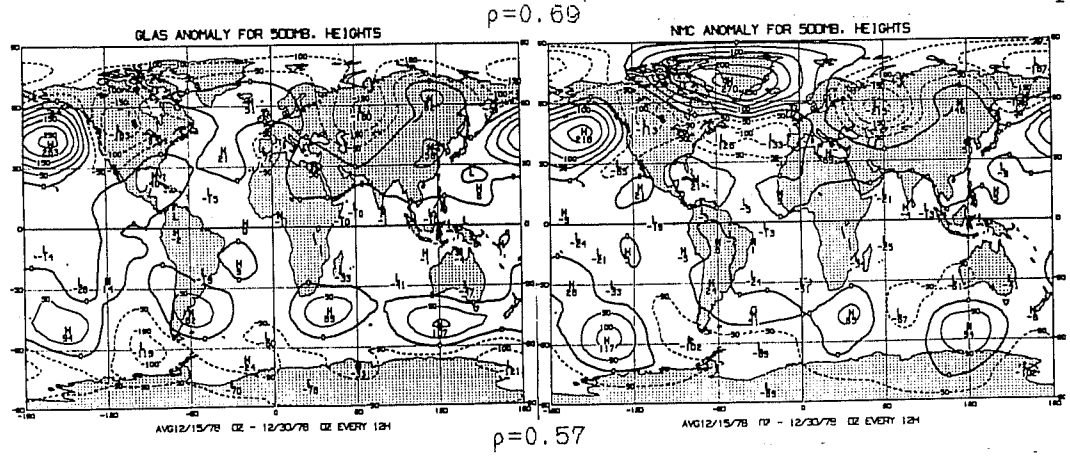

ρ=0.57

ρ=0.56

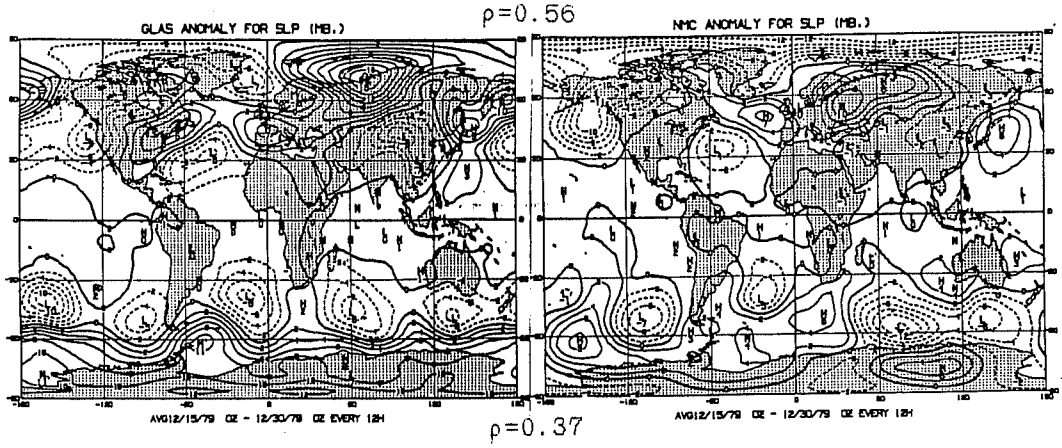

ρ=0.37

15/12/79-30/12/79

Fig. 2.4

ρ=0.77

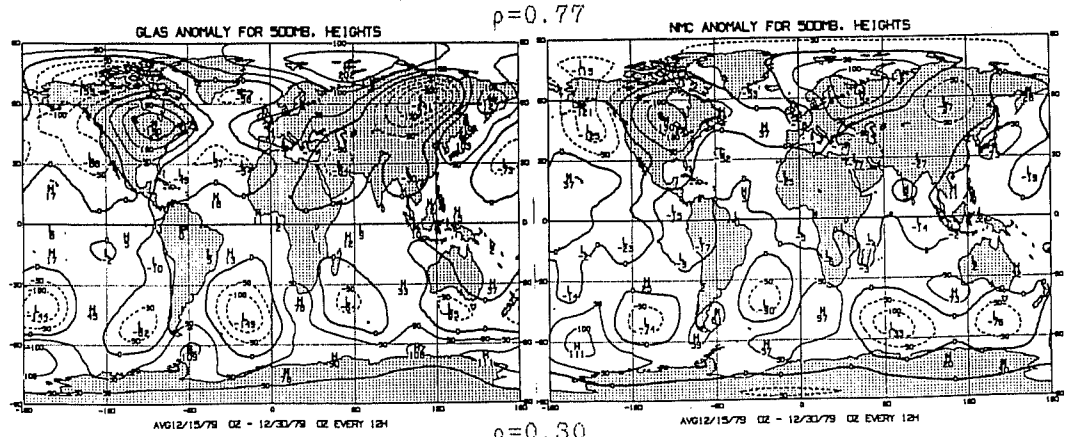

ρ=0.30

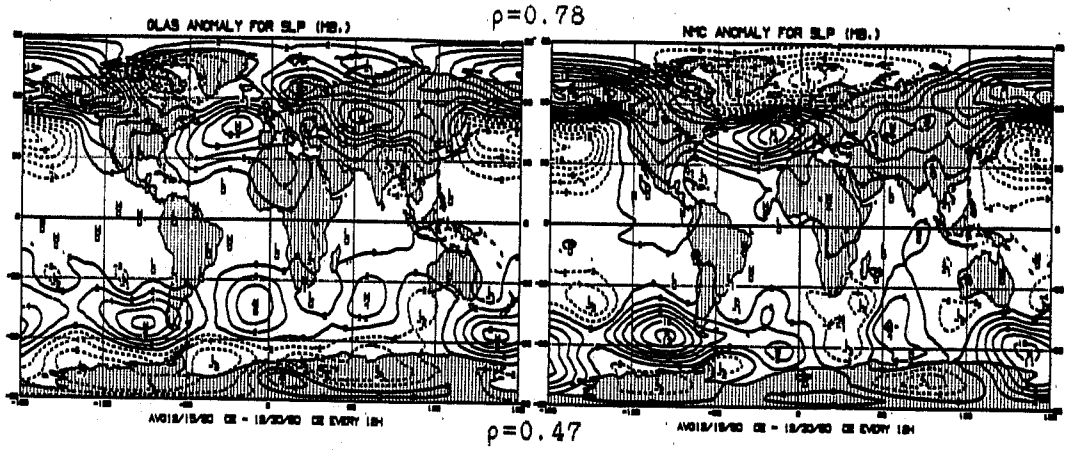

ρ=0.78

ρ=0.47

15/12/80-30/12/80

Fig. 2.5

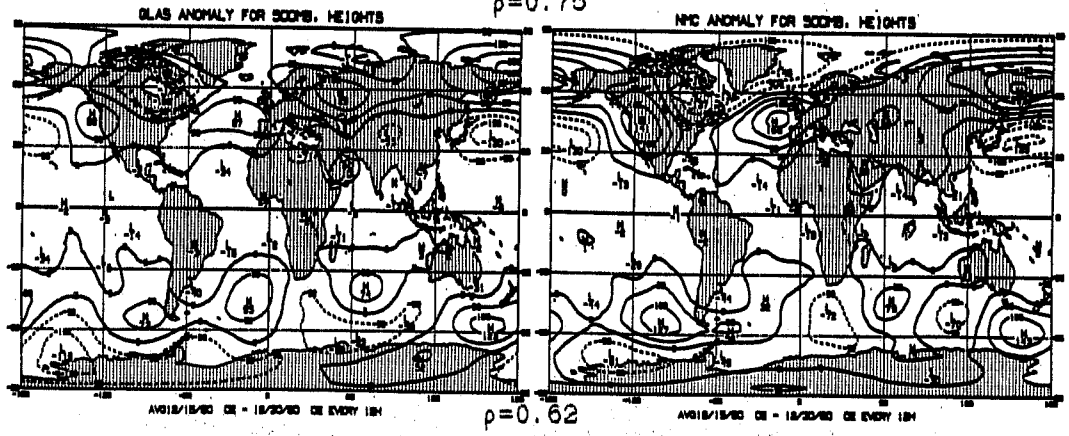

ρ=0.62

ρ=0.31

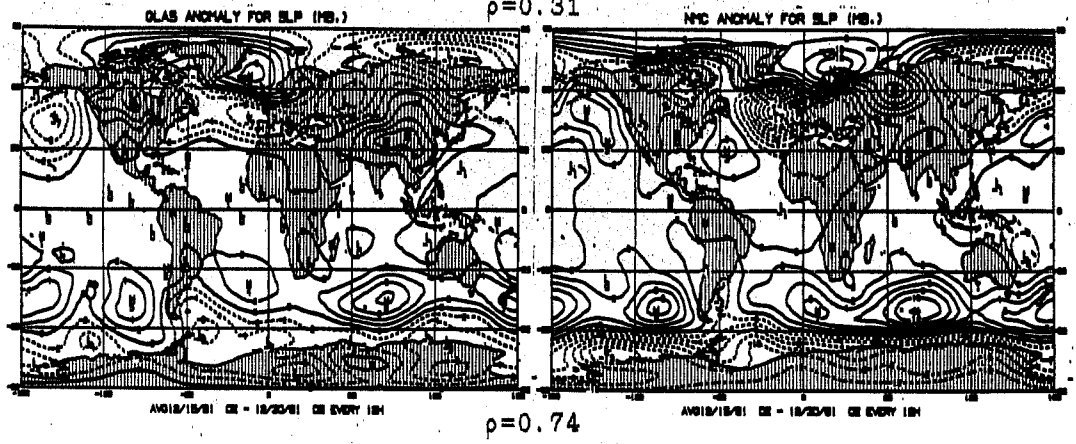

ρ=0.74

15/12/81-30/12/81

Fig. 2.6

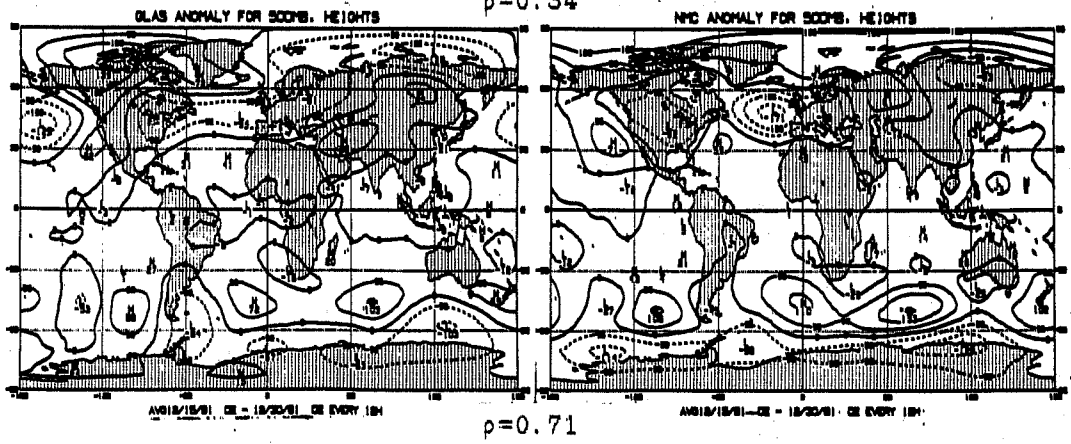

ρ=0.34

ρ=0.71

ρ=0.51

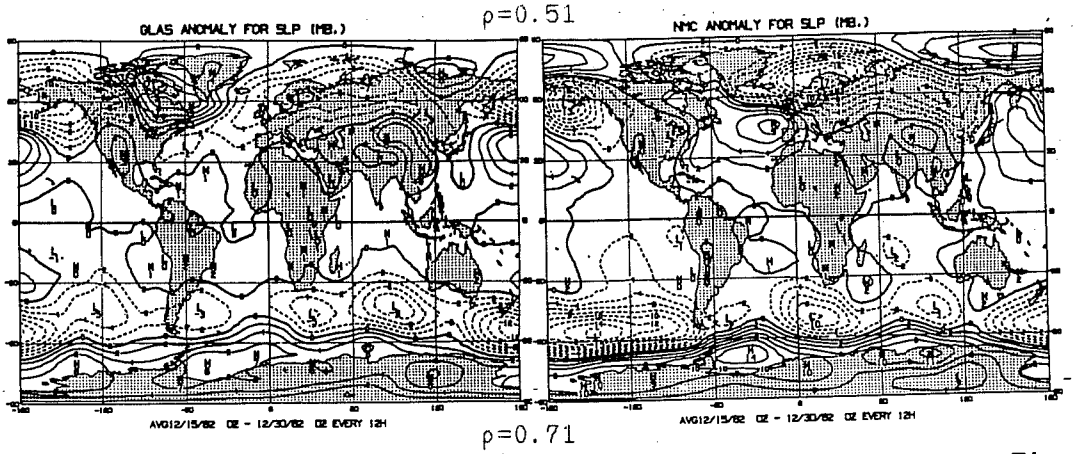

ρ=0.71

15/12/82-30/12/82

Fig. 2.7

ρ=0.52

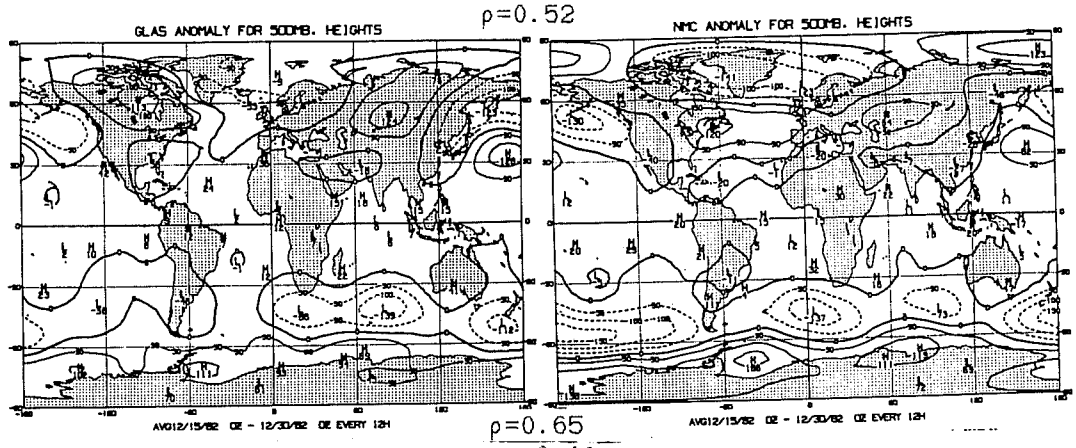

ρ=0.65

ρ=-0.01

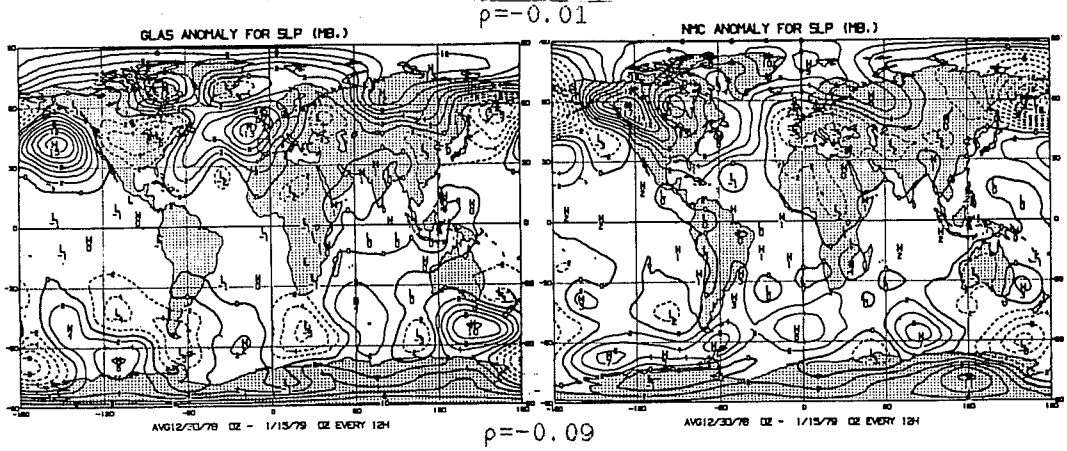

ρ=-0.09

31/12/78-15/1/79

Fig. 2.8

ρ=-0.19

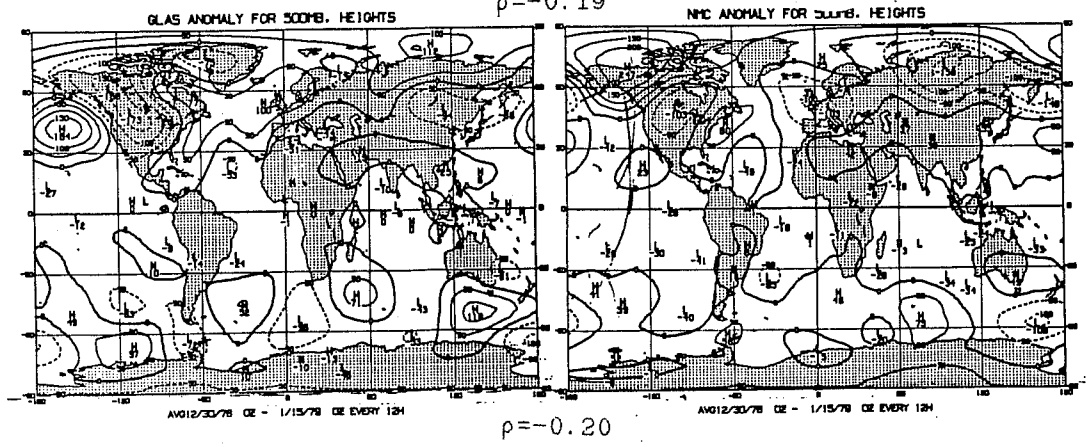

ρ=-0.20

ρ=0.35

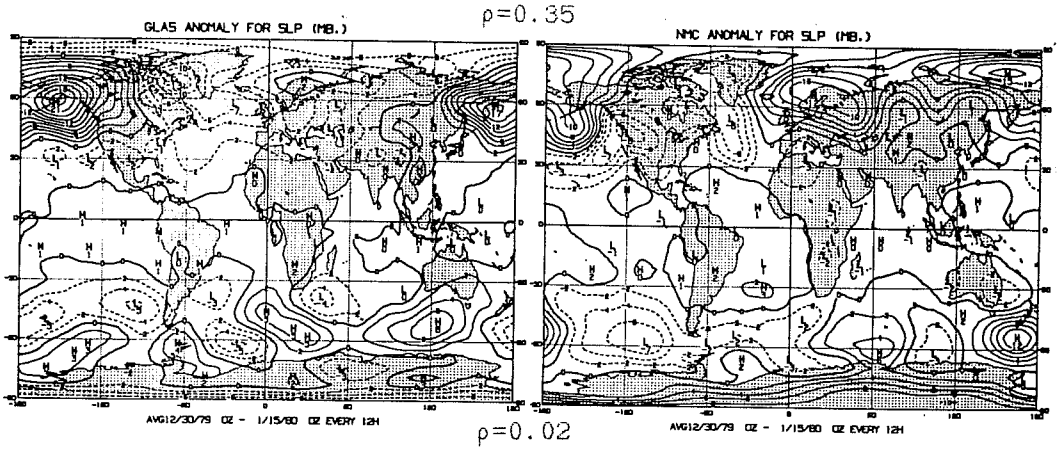

ρ=0.02

31/12/79-15/1/80

Fig. 2.9

ρ=0.02

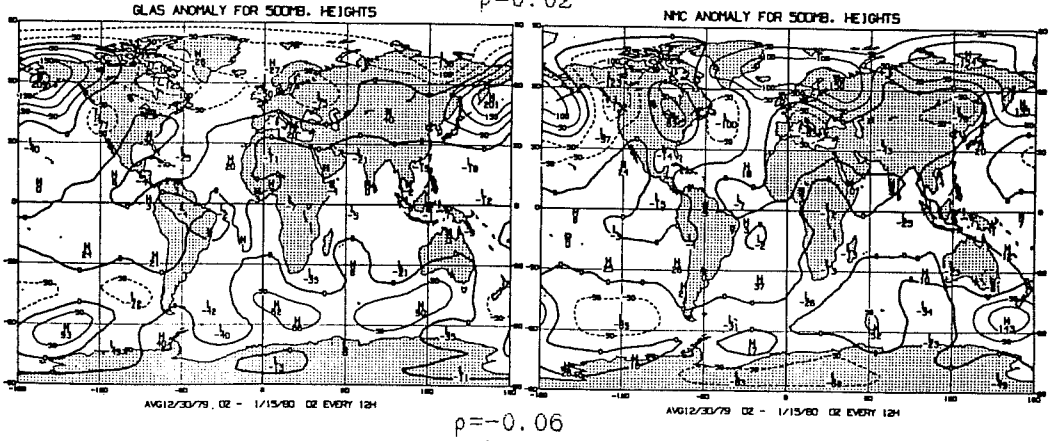

ρ=-0.06

ρ=0.47

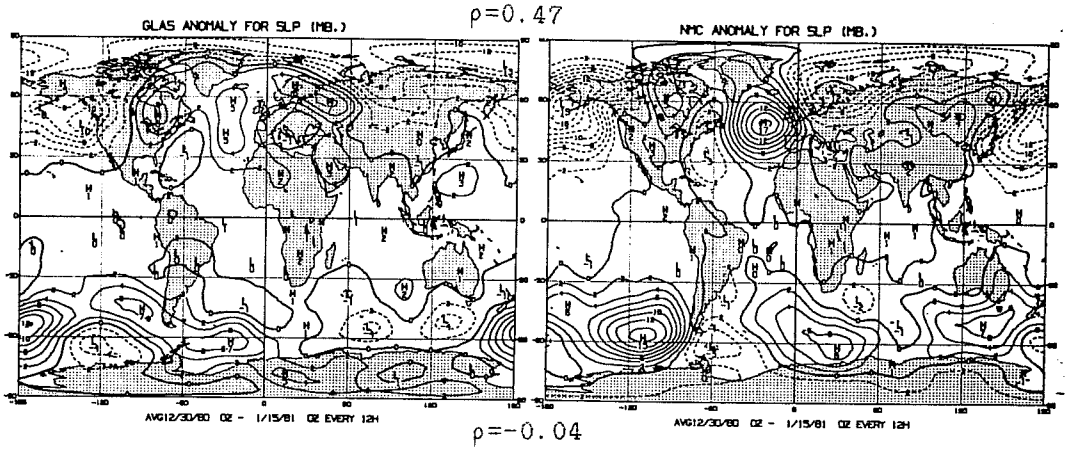

ρ=-0.04

31/12/80-15/1/81

ρ=0.40

Fig. 2.10

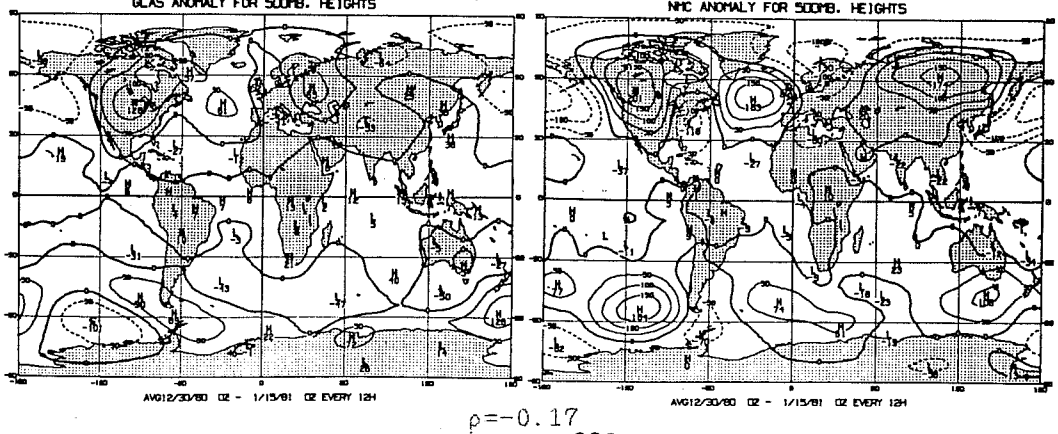

ρ=-0.17

ρ=-0.43

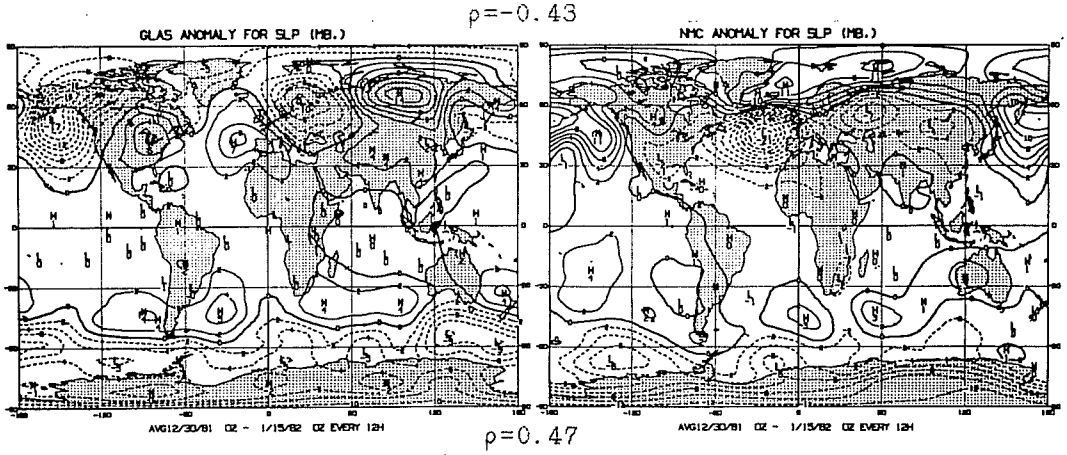

ρ=0.47

31/12/81-15/1/82

Fig. 2.11

ρ=-0.48

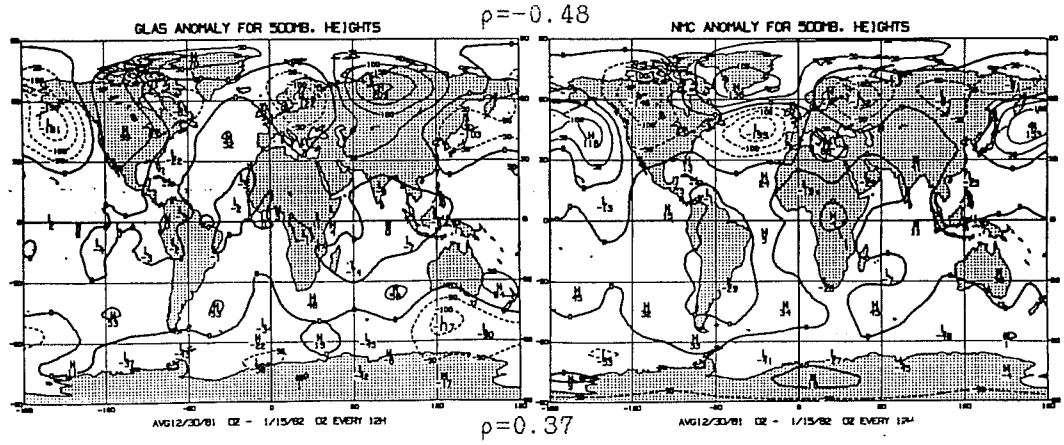

ρ=0.37

ρ=-0.26

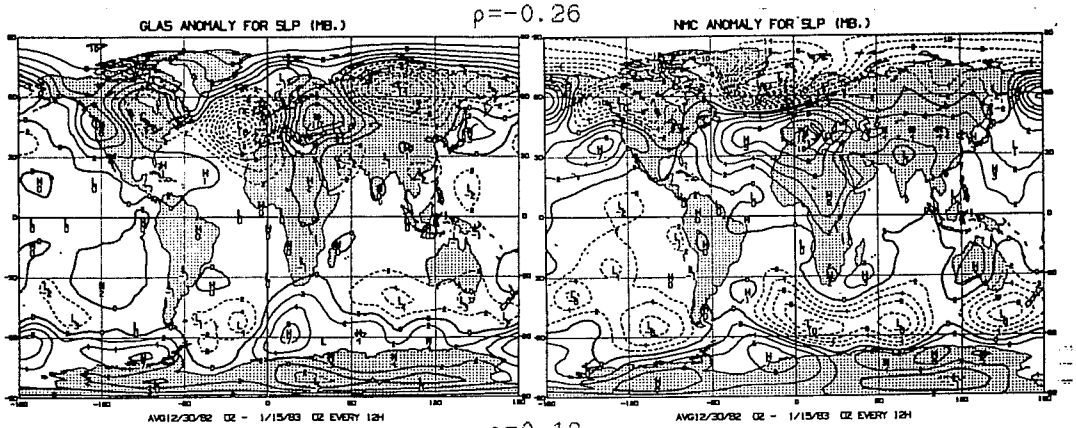

ρ=0.13

31/12/82-15/1/83

Fig. 2.12

ρ=-0.21

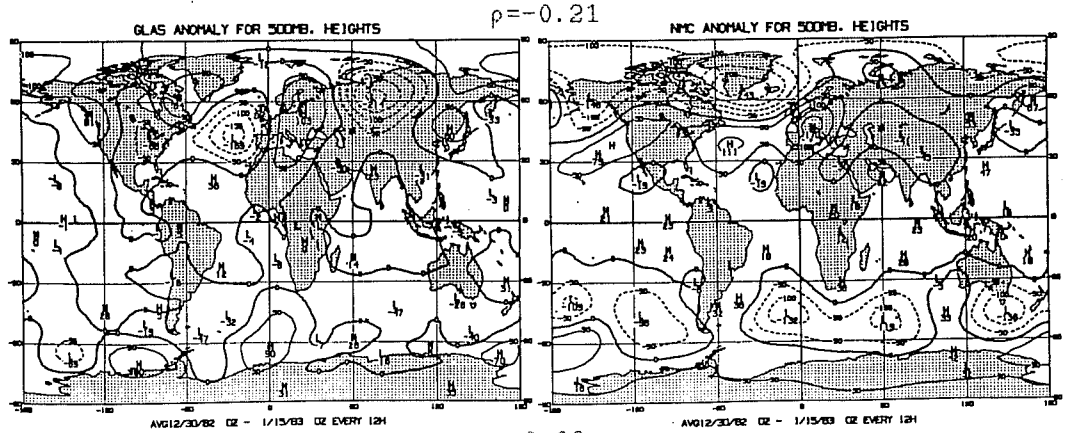

ρ=0.06

3. FORECASTING FORECAST SKILL

Forecast skill in both short and long range predictions varies from case to case, from region to region, and depends on other factors such as season, weather regime, and the type of boundary anomalies. Given the smallness of the predictive skill that may be expected beyond the first week of the dynamic predictions, it is imperative to devote considerable effort in estimating the skill of LRF's on a case-to-case basis.

In an application of LAF to operational ECMWF forecasts, Dalcher et al. (1985) found that although LAF showed marked improvements upon the operational dynamical forecasts, the success in predicting individual forecast skill was only minimal. They attributed this lack of success to the use of global verifications which could have masked regional variations in skill.

Recently, Kalnay and Dalcher (1986a, denoted KD from now on), have had considerable success in predicting skill using ensemble forecasting with regional verifications. Although their results were derived using medium range forecasts (5-days long), they suggest that similar techniques could be applied using LAF on long range forecasts. They used as a data base 5 sets of analysis/forecasts denoted "FGGE", "NOSAT", "NOTEMP", "NOWIND", and "NOCTW", previously derived at GLA for satellite data impact studies (Halem, et al., 1982, Kalnay, et al., 1985).

Because of the relatively large data density in the N.H., it was observed that the analyses generally tend to resemble each other, and therefore N.H. forecasts derived from the five different analyses can be considered as

members of an ensemble of forecasts whose initial conditions have been moderately perturbed. In this study, KD verified forecasts from the last four analyses against the forecast from the FGGE analysis. The average anomaly correlation of forecasts versus forecast (denoted R), was then used to predict the anomaly correlation of the FGGE forecasts verified against the ECMWF analysis (denoted ρ). The verifications of 14 forecasts were performed over four regions of the Northern Hemisphere (North America, Europe, North Pacific and North Atlantic), both for sea level pressure and 500 mb. Figure 3.1 presents both R (forecast/forecast average anomaly correlation) and ρ(forecast/analysis anomaly correlation) for the forecast of 21 January 1979, a case already studied by other groups. It is remarkable that in three forecasts that remained skillful throughout the 5 days ($\rho > 0.6$), the forecasts also remained close to each other ($R \gtrsim 0.9$), whereas in the SLP forecast over North America, which failed after less than 3 days, there was also considerable dispersion among the forecasts ($R \lesssim 0.8$).

This suggests that, on a regional basis, R can be used to predict ρ. This is confirmed by the contingency Table 3.1, in which for the vast majority of regional forecasts, the breakdown in skill (i.e., the time at which ρ crosses 60%) was correctly predicted to take place after 5 days or before 5 days. When the verifications were performed on the whole N.H., there was no useful a priori discrimination of forecast skill (Tables 3.2 and 3.3).

KD then determined a relationship between ρ and R with the following procedure: For each value of R, the median time of crossing, T, is the time that it took half of the forecast/forecast correlations to reach

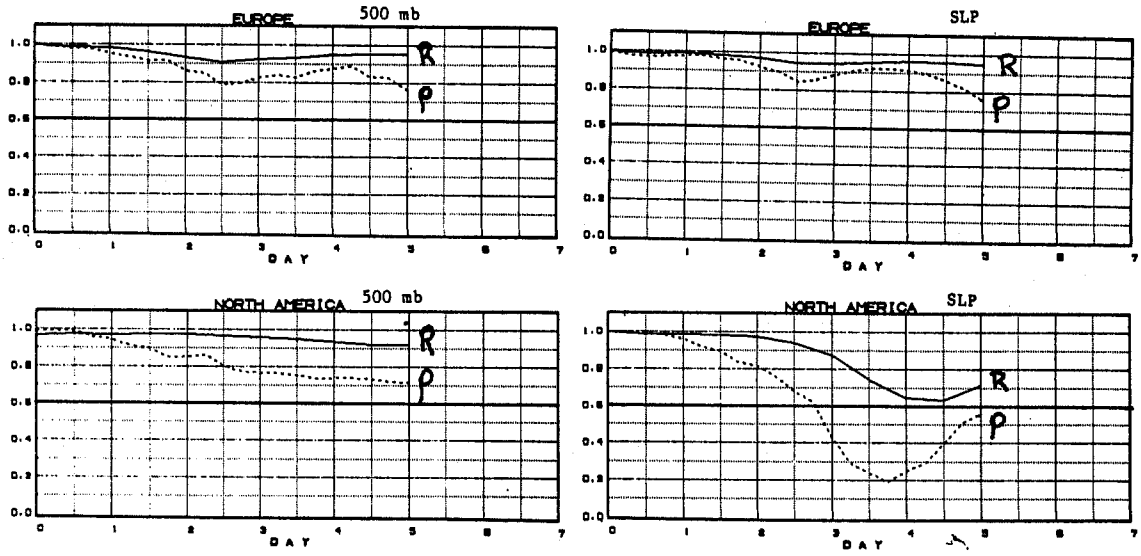

Fig. 3.1: Forecast/analysis anomaly correlation (ρ) and average forecast/forecast correlation (R) for the forecast from 21 Jan 1979, verified over Europe and North America, SLP and 500 mb.

>5 days observed breakdown	55	11
<5 days	7	39
	>5 days predicted breakdown	<5 days predicted breakdown

Table 3.1: Contingency table indicating the proportion of forecasts which remained skillful (ρ≥0.60) for more than five days among those predicted to remain skillful beyond five days. The table includes 14 forecasts verified over four regions, both at 500 mb and sea level pressure (SLP).

8	4	
2	14	

North America

14	1	
2	11	

Europe

19	1	
2	6	

North Atlantic

14	5	
1	8	

North Pacific

Table 3.2: Same as Table 3.1 but for the individual verification regions.

11	7	
7	3	

Northern Hemisphere

Table 3.3: Same as Table 3.1 but for the whole extratropical Northern Hemisphere.

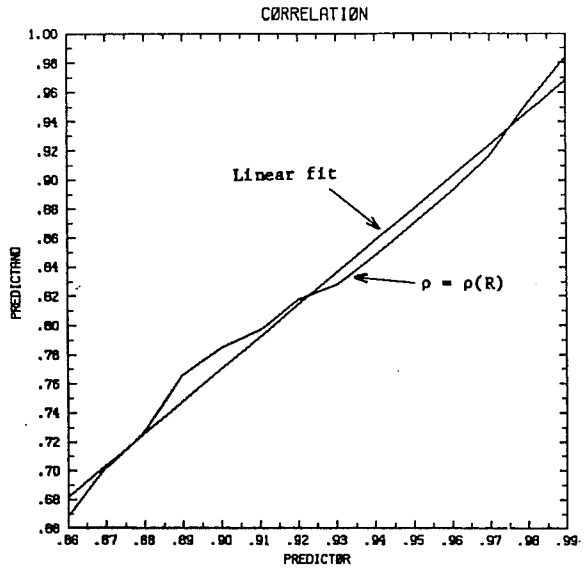

Fig. 3.2:

Relationship between the average forecast/forecast correlation R and the forecast/analysis correlation ρ derived using the median method, and its linear fit.

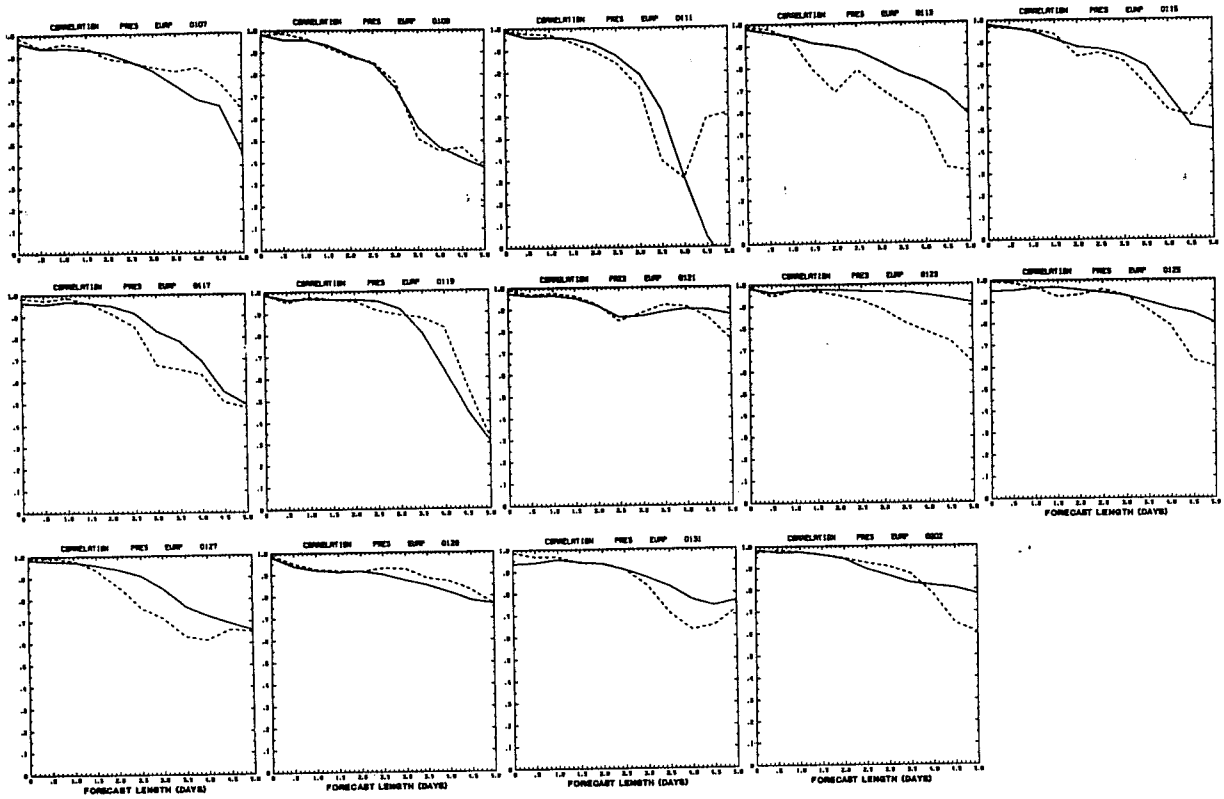

Fig. 3.3: Predicted (full lines) and observed (dashed) sea level pressure anomaly correlations for each of the fourteen forecasts verified over Europe.

the value R. The median forecast/analysis correlation ρ was then determined such that at time T half of the forecasts had not yet reached ρ. Figure 3.2 presents the derived ρ(R) relationship and its linear fit. The linear fit, $\rho = 2.2\ R - 1.2$, extrapolated for values of ρ less than 0.68, was then used to predict the forecast/analysis anomaly correlation. Figure 3.3 presents the observed anomaly correlation ρ and the predicted ρ(R) for all 14 sea level pressure forecasts over Europe. Although there are several cases of overly optimistic or pessimistic forecasts, it is clear that this method has the potential of providing a case-to-case a priori estimation of skill.

4. CASE STUDIES OF PERSISTENT WEATHER ANOMALIES

We have performed three case studies of long-lasting severe weather anomalies with the purpose of both to explore their predictability and to determine their origin. The first one was devoted to the 1980 summer heat wave over the U.S., and the other two were studies of long-lasting phenomena in the Southern Hemisphere.

4.1 Experiments on the Summer 1980 U.S. Heat Wave

In the summer of 1980, a prolonged heat wave affected the U.S. While the heat was most persistent in the Great Plains, nearly the entire country experienced abnormally warm weather. At GLA, a number of studies have been performed to study the mechanisms and predictability of the heat wave (Atlas, et al., 1985; Wolfson and Atlas, 1986; Wolfson et al., 1986). A heat wave index (HWI) was developed taking into account the two important factors of intensity and persistence which is highly correlated to the surface air temperature on different time scales. The GLA Fourth Order GCM was used in two experimental 130-day long integrations, for

1979 and 1980, and in a series of 10-day integrations designed to assess the role of boundary forcing in the maintenance and decay of the heat wave.

Figure 4.1 presents observed and forecasted HWI values average over 13 consecutive 10-day periods started on 15 May 1980 and 1979. In both years there seems to be some skill in predicting the evolution of this index of persistent anomalies for about four to five 10-day periods. The rapid change of the circulation between May and June 1980 is also well captured. Maps of the June and July observed and forecasted index divided by the daily standard deviation confirm this result (Fig. 4.2). Shorter experiments indicated that lower than normal soil moisture over the U.S. contributed to the maintenance of the wave by reducing evaporation and increasing surface sensible heat fluxes, whereas SST anomalies tended to reduce the intensity of the heat wave, but these effects were secondary to dynamical effects.

4.2 Large-Amplitude Stationary Waves Near South America During January 1979

One of the most remarkable anomalies of the FGGE year were very large-amplitude stationary waves, of a zonal wavenumber ~7 that persisted for more than a month during the end of December and throughout January 1979 near South America (Fig. 4.3a).

These waves were studied by Kalnay et al. (1986) using the GLA Fourth order GCM which provided a reasonable control forecast (Fig. 4.3b). Through mechanistic experiments and theoretical analysis they showed that the waves were not due to orographic forcing by the Andes or to SST anomalies.

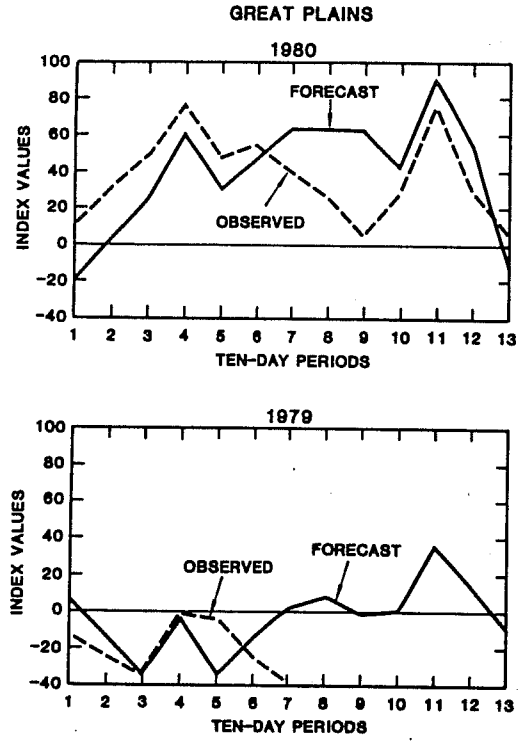

Fig. 4.1:

Observed and predicted heat wave index in 1979 and 1980.

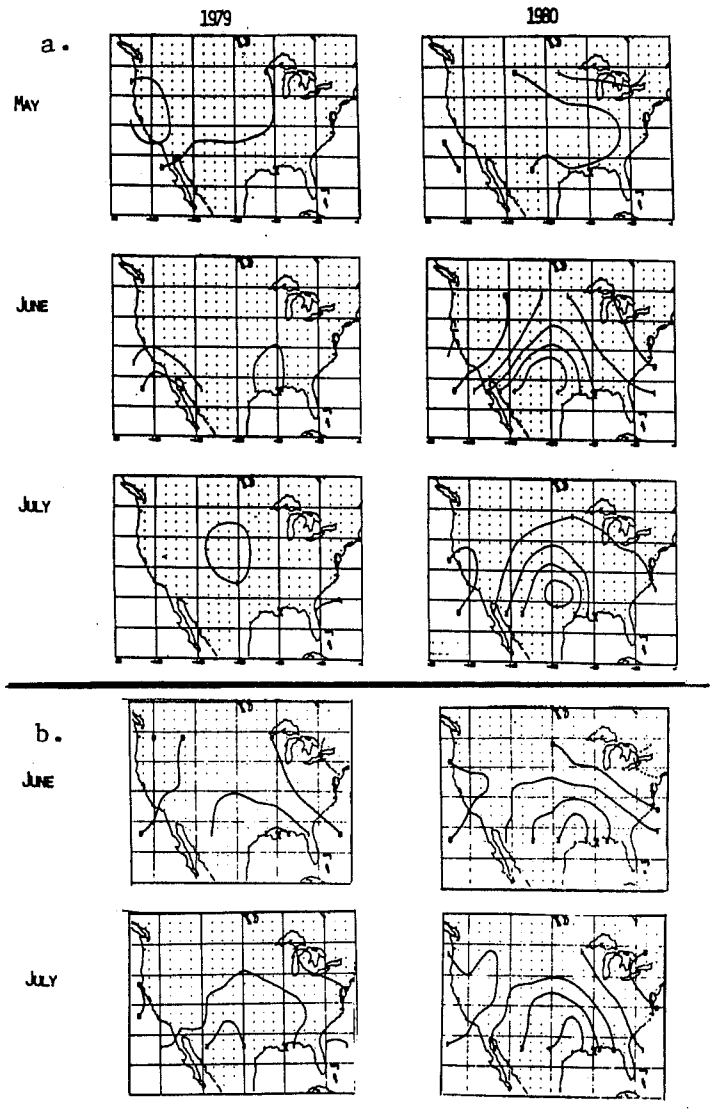

Fig. 4.2a:

Observed t-index over U.S. during May, June of 1979 and 1980.

Fig. 4.2b:

Predicted t-index for June, July of 1979 and 1980.

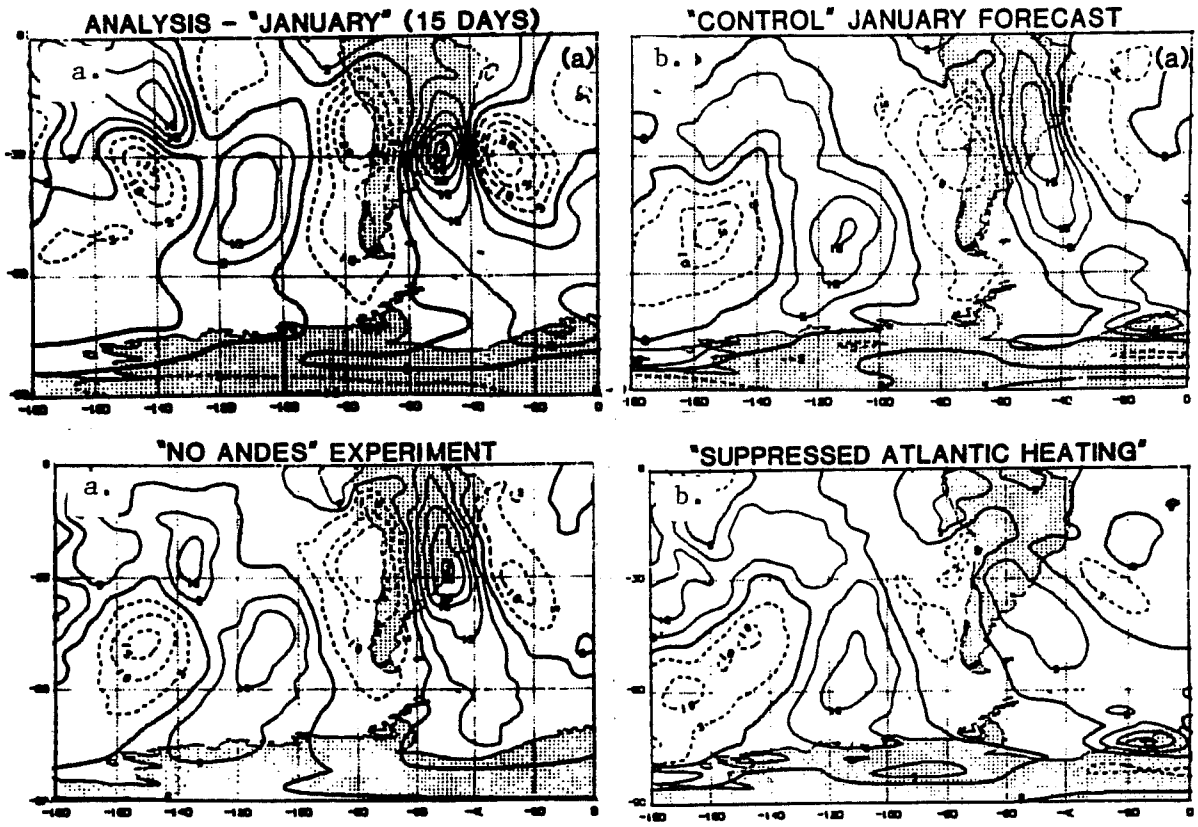

Fig. 4.3 and 4.4 (above)

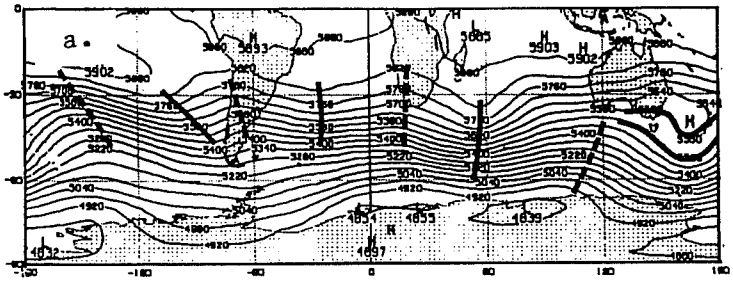

OBSERVED 500 MB HEIGHTS AVERAGED OVER 8-23 JUNE 1982

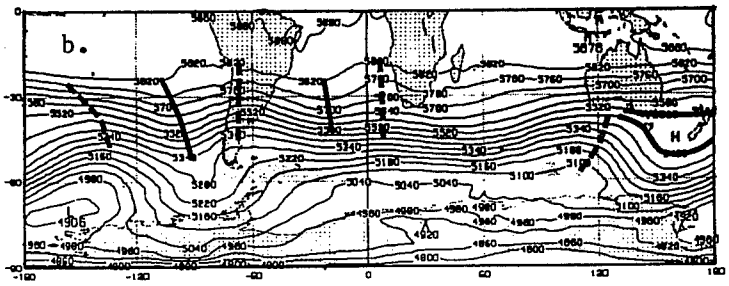

15 DAY AVERAGED FORECAST FROM 8 JUNE 1982. GLA MODEL WITH CLIMATOLOGICAL SST.

Fig. 4.5

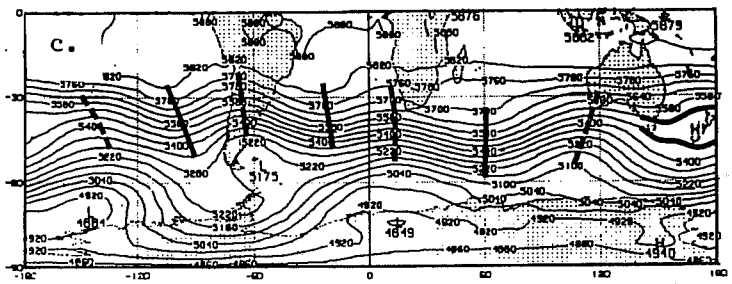

15 DAY AVERAGED FORECAST FROM 8 JUNE 1982. GLA MODEL WITH JUNE 1982 SST.

They found that they were associated with tropical heating, local convective heating, and to the intensity and position of the South Pacific Convergence Zone (Fig. 4.4).

4.3 A GCM Study of the Maintenance of the June 1982 Blocking in the S.H.

Mo et al. (1986) studied the June 1982 blocking ridge in the Australian-New Zealand region which persisted for 15 days. They performed a control forecast and several mechanistic experiments modifying the orographic forcing, SST, latent heating, surface fluxes, land-sea properties and initial conditions of the planetary waves.

Figure 4.5 show that the control forecast succeeded in predicting the maintenance of the blocking ridge at 160E. An experiment with observed SST anomalies confirmed their theoretical argument that the Pacific SST anomalies were driven by and provide a negative feedback to the atmospheric anomalies. The use of real SST's resulted in an improved forecast of the ridge in the South Indian ocean but it weakened the New Zealand blocking (Fig. 4.5c).

Other conclusions of this study were that orographic forcing has only local influence on the winter circulation of the SH, and no effect on the New Zealand blocking, and that the block was not a response to tropical or monsoonal heating. Three experiments showed that the most important boundary forcing associated with the maintenance of the block is the heating due to land-sea contrast. Local heating in the Australian region and high latitude sensible heating due to cold air outbreaks from Antarctica contribute significantly to the persistence of the block.

5. RELATIONSHIP BETWEEN SST AND PRECIPITATION ANOMALIES

Suarez (1986) has performed a study of the effect of the 1982-1983 El Nino SST anomalies on the atmospheric circulation. He used his 2-level, 4° lat by 5° lon GCM, which is about 100 times faster than the GLA 9-level model, and still retains the ability to reproduce rather well many atmospheric circulation characteristics. Fig. 5.1 presents the predicted precipitation anomaly as well as the observed outgoing long-wave radiation (OLR) anomaly. A comparison of Figs. 5.1 and 5.2 indicates that although the anomaly in evaporation is closely related to the SST anomaly, both positive and negative precipitation anomalies are much stronger and distributed in different regions. Suarez has developed a theory that takes into account the amplifying effect of the positive feedback between evaporation, precipitation and convergence of water vapor. The theory results in a multiplying factor which depends only on the thermodynamic state of the atmosphere and not on the wind distribution, which is harder to measure. The multiplying factor, S/M (Fig. 5.3) can then be used to determine the expected precipitation anomaly from the SST anomalies and from the expected thermodynamic state of the atmosphere.

6. SCALE-DEPENDENCE OF ERROR GROWTH AND DYNAMIC PREDICTABALITY

Kalnay and Dalcher (1986b) studied the forecast error growth in the 100-day ECMWF data set of 10-day forecasts previously utilized by Lorenz (1982). They extended Lorenz' model for error growth by including the effect of errors associated with deficiencies in the forecast model, and applied the new parameterization to the error variance of the 10-day forecasts (Fig. 6.1). They showed that the commonly used parameter "doubling time of small errors" is not a good measure of error growth because it is very sensitive to the method of extrapolation to small errors.

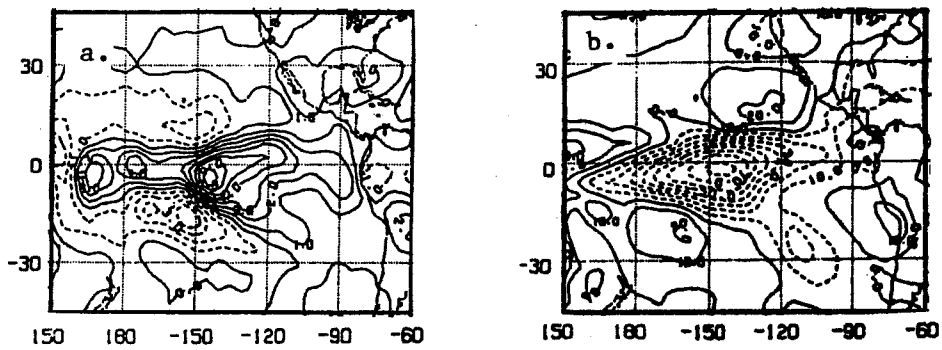

Fig. 5.1a: Predicted precipitation anomaly. Cont. int., 1 mm/day.

b: Observed OLR anomaly. Cont. int. 10 w/m^2.

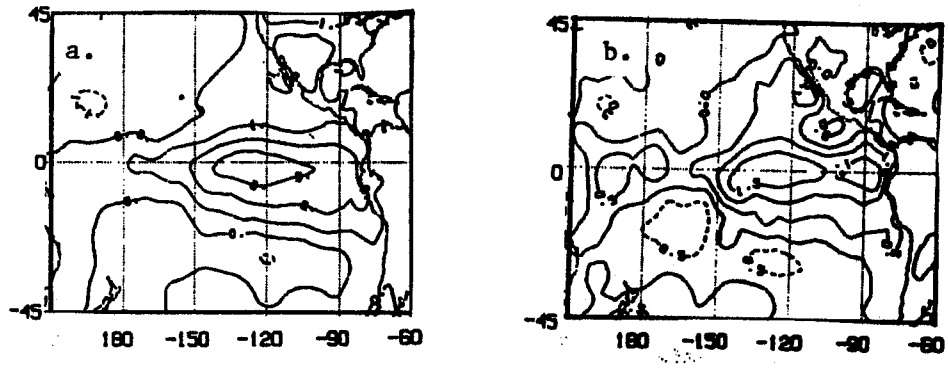

Fig. 5.2a: SST anomaly. Cont. int. 1°K.

b: Predicted evaporation anomaly δE. Cont. int. 0.5 mm/day.

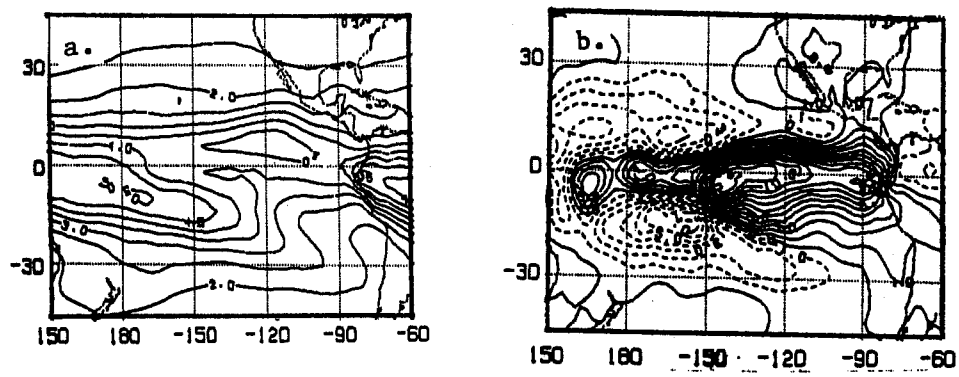

Fig. 5.3a: Theoretical amplification factor S/M. Contour interval: 1.

b: Derived precipitation anomaly δ(S/M.E). Contour interval: 1 mm/day.

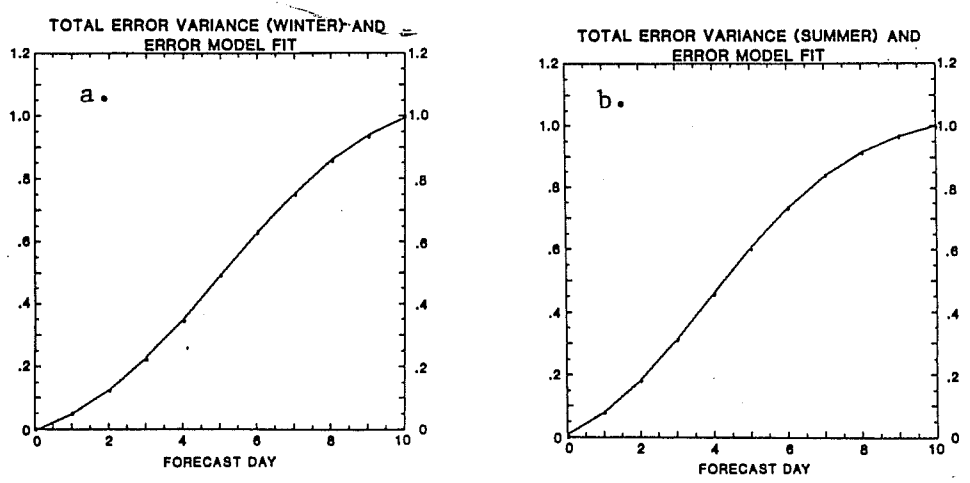

Fig. 6.1: Total error variance growth. Observed (points) and fitted model (curve).
a) winter [Scaled by .97 . 10^6 $(g.m.)^2$]
b) summer [Scaled by .89 . 10^6 $(g.m.)^2$]

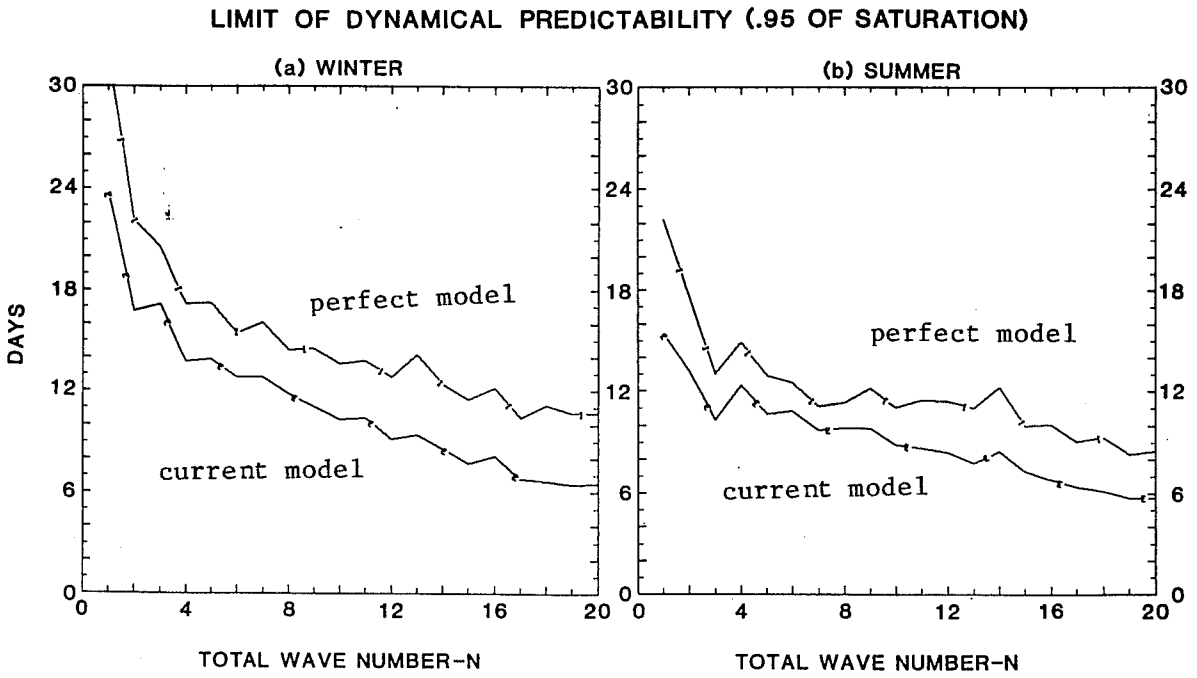

Fig. 6.2: Limit of dynamic predictability defined as the time at which forecast error reaches 95% of the error saturation value. The lower curve corresponds to the current model, and the upper curve to a perfect model. a) Winter; b) Summer

They also fitted the error to each 2-dimensional total wavenumber n and concluded that the rate of growth of errors increases with wavenumber and that the saturation error variance decreases with wavenumber.

In addition, Kalnay and Dalcher (1986b) showed that the limit of dynamic predictability, which they defined as the time at which error variance reaches 95% of saturation, decreases monotonically with n (Fig. 6.2). In the winter, waves with $n \lesssim 8$ have not yet reached 95% of saturation at 10 days. A perfect model with error growth similar to the present model would reach a 3 week limit of predictability for $n \lesssim 4$. In the summer, error growth rates are larger than in winter, and even for the low wavenumbers in a perfect model, the limit of predictability is closer to two weeks.

7. OTHER CURRENT RELATED RESEARCH

Several other related research projects are currently in progress at GLA. Because of the lack of space we limit ourselves to a list of some of the projects and of the scientists involved in them.

a) Diagnostic Studies of Extratropical Quasi-Stationary Flow Patterns, and Their Relationship to Tropical Forcing (Livezey and Mo)

b) Correction and Prediction of Model Error for Extended and Long-Range Prediction with Regime Emphasis (Livezey and Schemm)

c) GLA Fourth Order Model Development
   - High resolution (Pfaendtner and Helfand)
   - Gravity wave drag parameterization (Helfand, Jusem, Pfaendtner)
   - Cumulus parameterization (Sud, Helfand, Mintz)
   - High order closure PBL parameterization (Helfand and Jusem)
   - Simple Biosphere parameterization (Sellers, Mintz, Sud)

d) Effect of land and sea surface anomalies on the African drought (Sud and Semazzi)

e) Coupled ocean-atmosphere model (Suarez and Schopf)

f) Use of GLA Analysis/Forecast System to infer actual precipitation (Mintz et al.).

8. ACKNOWLEDGEMENTS

We gratefully acknowledge support for this research from the Atmospheric Dynamics and Radiation Branch of NASA Headquarters. The manuscript was prepared by Benita Richardson, and the figures in Section 2 by W. Smith and J. Ardizzone.

9. REFERENCES

Atlas, R., N. Wolfson, and Y. Sud, 1985: A numerical investigation of the summer 1980 heat wave on weather prediction. Proceedings of the 7th AMS Conference on Numerical Weather Prediction.

Baker, W. E., 1983: Objective analysis and assimilation of observational data for FGGE. Mon. Wea. Rev., 111, 328-342.

Baker, W. E., S. C. Bloom, J. S. Woollen, M. S. Nestler, Y. Brin, T. W. Schlatter, and G. W. Branstator, 1986: Experiments with a three-dimensional statistical objective analysis scheme using FGGE data. Mon. Wea. Rev. (In press).

Dalcher, A., E. Kalnay, R. Livezey and R. N. Hoffman, 1985: Medium Range Lagged Average Forecasts. Preprints from the Ninth AMS Conference on Probability and Statistics in Atmospheric Sciences. Virginia Beach, October 1985, pp. 130-136.

Halem, M., E. Kalnay-Rivas, W. E. Baker, and R. Atlas, 1982: An assessment of the FGGE satellite observing system during SOP-1. Bull. Amer. Meteor. Soc., 63, 407-426.

Hoffman, R., and E. Kalnay, 1983: Lagged average forecasting: An alternative to Monte Carlo forecasting. Tellus, 35A, 100-118.

Kalnay, E., R. Atlas, W. Baker and J. Susskind, 1985: GLAS experiments on the impact of FGGE satellite data on NWP. Proc. of First Nat. Workshop on the Global Weather Experiment. Nat. Acad. of Science Press, pp. 121-145.

Kalnay, E., R. Balgovind, W. Chao, D. Edelmann, J. Pfaendtner, L. Takacs and K. Takano, 1983: Documentation of the GLAS fourth order general circulation model. NASA Tech. Memo. 86064.

Kalnay, E., and A. Dalcher 1986a: Forecasting forecast skill. Submitted to Mon. Wea. Rev.

Kalnay, E., and A. Dalcher, 1986b: Error growth and predictability in operational ECMWF forcasts. Submitted to Tellus.

Kalnay, E., K. C. Mo, and J. Paegle, 1986: Large amplitude stationary waves in the Southern Hemisphere: Observations and mechanistic experiments to determine their origin. J. Atmos. Sci., 43, pp. 252-275.

Mo, K. C., J. Pfaendtner, and E. Kalnay, 1986: GCM experiments on the maintenance of the blocking of June 1982. Submitted to J. Atmos. Sci.

Reuter, D., and J. Susskind, 1985: Retrieval of sea-surface temperatures from HIRS2/MSU. J. Geophys. Res., 90C, 11, 602-11, 608, 1985.

Suarez, M., 1986: Analysis of a GCM's response to tropical SST anomalies. In preparation.

Susskind, J., J. Rosenfield, D. Reuter, and M. T. Chahine, 1984: Remote sensing of weather and climate parameters form HIRS2/MSU on TIROS-N. J. Geophys. Res., 89D, 4657-4676, 1984.